On calculations of metastable and Rydberg states of diatomic beryllium molecule and antiprotonic helium atom

Derbov, V., Chuluunbaatar, G., Gusev, A., Chuluunbaatar, O., Vinitsky, S., et al.

V. L. Derbov, G. Chuluunbaatar, A. A. Gusev, O. Chuluunbaatar, S. I. Vinitsky, A. Góźdź, P. M. Krassovitskiy, A. V. Mitin, "On calculations of metastable and Rydberg states of diatomic beryllium molecule and antiprotonic helium atom," Proc. SPIE 11458, Saratov Fall Meeting 2019: Laser Physics, Photonic Technologies, and Molecular Modeling, 114580Q (9 April 2020); doi: 10.1117/12.2565816

SPIE.

Event: Saratov Fall Meeting 2019: VII International Symposium on Optics and Biophotonics, 2019, Saratov, Russian Federation

On calculations of metastable and Rydberg states of diatomic beryllium molecule and antiprotonic helium atom *

V.L. Derbov[a], G. Chuluunbaatar[b,c], A.A. Gusev[b], O. Chuluunbaatar[b,d], S.I. Vinitsky[b,c], A. Góźdź[e], P.M. Krassovitskiy[a,f], and A.V. Mitin[g,h]

[a]N.G. Chernyshevsky Saratov National Research State University, Saratov, Russia
[b] Joint Institute for Nuclear Research, Dubna, Russia
[c] Peoples' Friendship University of Russia (RUDN University), 117198 Moscow, Russia
[d] Institute of Mathematics, National University of Mongolia, Ulaanbaatar, Mongolia
[e] Institute of Physics, University of M. Curie-Skłodowska, Lublin, Poland
[f]Institute of Nuclear Physics, Almaty, Kazakhstan
[g] Moscow Institute of Physics and Technology, Dolgoprudny, Moscow Region, Russia
[h] Joint Institute for High Temperatures of RAS, Moscow, Russia

ABSTRACT

The computational scheme and calculation results of bound, metastable and Rydberg states of atomic and molecular systems important for laser spectroscopy are presented. The solution to the problem is performed using the authors' software package (see program libraries of the Computer Physics Communications journal and of the Joint Institute for Nuclear Research) that implement the high-accuracy finite element method. The FORTRAN procedure of matching tabulated potential functions with van der Waals asymptotic potential using interpolation Hermite polynomials which provides continuity of both the function itself and its derivative is presented. The efficiency of the proposed approach is demonstrated by calculated for the first time sharp metastable states with complex eigenenergies in a diatomic beryllium molecule and weakly bound Rydberg states of antiprotonic helium atom.

Keywords: laser spectroscopy, eigenvalue problem, bound and metastable states, finite element method, diatomic beryllium molecule, vibration-rotation states, antiprotonic helium

1. INTRODUCTION

During last decade the theoretical investigations[1–5] have shown 12 vibrational bound states in a diatomic beryllium molecule, whereas 11 states were extracted from the experimental data of laser pump-probe spectroscopy (see Fig. 1 in Ref. 6). Earlier[7] we started to study the vibration-rotational spectrum of diatomic beryllium molecule. We solved the boundary value problem (BVP) for the second-order ordinary differential equation (SOODE) with potential function numerically tabulated on a non-uniform grid in a finite interval of the independent variable values.[3] To formulate the BVP on a semiaxis, the potential function should be continued beyond the finite interval using the additional information about the interaction of atoms comprising the diatomic molecule at large interatomic distances. The leading term of the potential function at large distances is given by the van der Waals interaction, inversely proportional to the sixth power of the independent variable with the constant, determined from theory.[8,9] Proceeding in this way we faced a problem how to match the asymptotic expansion of the potential function with its tabulated numerical values (within the accuracy of their calculation) at a suitable sufficiently large distance.

In the present paper we continue studying this problem. Firstly, we present the results of calculating rotational-vibrational metastable states of diatomic beryllium molecule having complex eigenenergies. Next,

*The work was partially supported by the RFBR (grant No. 18-51-18005), the Bogoliubov-Infeld program, the Hulubei-Meshcheryakov program, the RUDN University Program 5-100 and grant of Plenipotentiary of the Republic of Kazakhstan in JINR.

Send correspondence to V.L.D.: E-mail: derbovvl@gmail.com, Telephone: +7 927 220 8353

Saratov Fall Meeting 2019: Laser Physics, Photonic Technologies, and Molecular Modeling, edited by Vladimir L. Derbov, Proc. of SPIE Vol. 11458, 114580Q · © 2020 SPIE
CCC code: 1605-7422/20/$21 · doi: 10.1117/12.2565816

Table 1. Comparison of the vibrational spectra $E_{v=0L=0} - E_{vL=0}$ (in cm^{-1}) for the $X_1\Sigma_g^+$ state of the beryllium dimer calculated by the KANTBP 4M[11] and ODPEVP[10] programs implementing FEM (FEM), ab initio MEMO calculation,[3] theoretical (EMO) and experimental (Exp) results,[6] symmetry-adapted perturbation theory (SAPT),[1] the Morse-long range (MLR) function and Chebyshev polynomial expansion (CPE)[5] and Slater-type orbitals(STO);[4] D_e is the well depth and D_0 is the dissociation energy in cm^{-1}, r_e is the equilibrium internuclear distance in Å, RMS is root-mean-square (RMS) dicrepancy between the theoretical and experimental data.

n	v	FEM	MEMO	EMO	Exp	SAPT	MLR&CPE	STO
	r_e	2.4534	2.4534	2.4535	2.4536	2.443	2.445	2.4344
	D_e	929.804	929.74	929.74	929.7±2	938.7	934.8	934.6±2.5
1	D_0	806.07	806.48	806.5	807.4	812.4	808.1510	807.7
2	1	222.50	222.16	222.7	222.6	222.3	222.9170	223.4
3	2	397.34	397.6	397.8	397.1	397.6	397.4191	400.1
4	3	517.71	517.87	518.2	518.1	520.3	518.4196	517.3
5	4	594.89	595.06	595.4	594.8	597.9	595.0856	595.1
6	5	651.91	652.10	652.4	651.5	655.1	651.7974	651.7
7	6	698.92	699.14	699.4	698.8	702.6	699.0308	698.7
8	7	737.72	737.97	738.2	737.7	741.7	737.9791	738.0
9	8	768.27	768.56	768.8	768.2	772.4	768.5002	769.3
10	9	789.74	790.05	790.7	789.9	794.3	790.1738	790.1
11	10	801.66	802.08	803.4	802.6	807.1	802.8323	802.6
12	11	805.74	806.21			811.9	807.5335	807.5
RMS		0.4	0.4	0.6		3.4	0.3	1.1

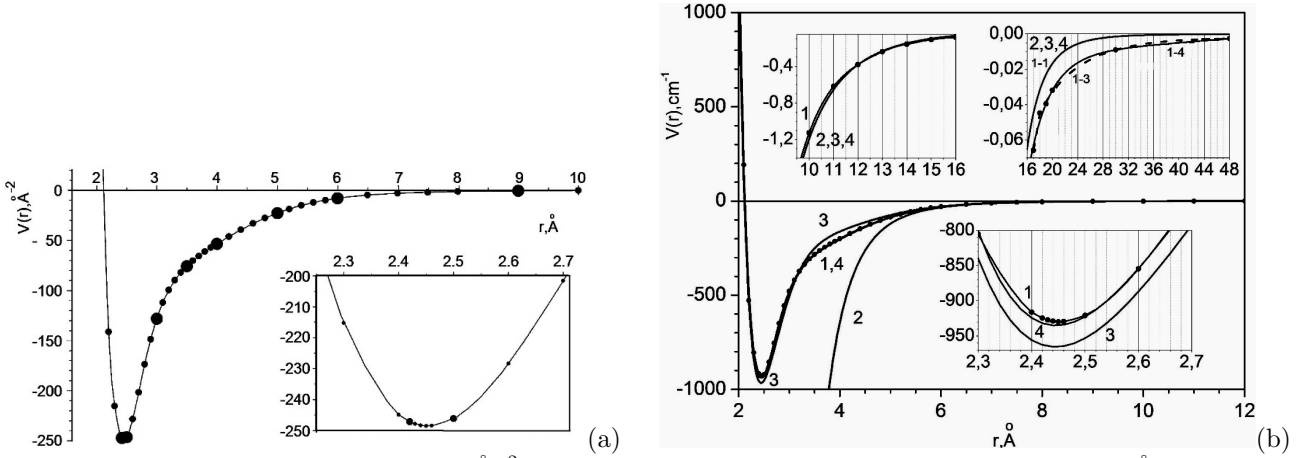

Figure 1. (a) The potential function $V(r)$ ($Å^{-2}$) of the beryllium diatomic molecule as a function of r (Å) obtained by interpolating the tabulated values[3] (points in the subintervals, the boundaries of which are larger-size points) by means of the fifth-order LIPs. (b) The MEMO potential function $V(r)$ (points and line 1[3]), the asymptotic expansion $V_{\rm as}(r)$ of the MEMO function (line 2,[9]), the analytical forms of the potential function $V_{an}(r)$ (line 3[8] and line 4[5]). r is given in Å, $V_*(r)$ in cm^{-1}.

we present our results for the weakly bound Rydberg states of antiprotonic helium atom. High-precision theoretical estimates are of significant importance for further experiments in laser spectroscopy of weakly bound systems. The development of technique for solving the above class of eigenvalue problems for the SOODE using the programs ODPEVP[10] and KANTBP 4M[11] implementing the finite element method[12,13] in Fortran and Maple, respectively, and the symbolic algorithm of the algebraic perturbation theory for a hydrogen-like atom in the field of a distant point charge[14] implemented as POINTFIELD program in REDUCE is also a subject of the present study.

2. BERYLLIUM DIATOMIC MOLECULE: BOUND AND METASTABLE STATES

In quantum chemical calculations, the effective potentials of interatomic interaction are presented in the form of numerical tables calculated with limited accuracy and defined on a nonuniform mesh of nodes in a finite domain of interatomic distance variation. However, for a number of diatomic molecules the asymptotic expressions for the effective potentials are calculated analytically for sufficiently large distances between the atoms. The equation for a diatomic molecule in the crude adiabatic approximation, commonly referred to as Born–Oppenheimer (BO)

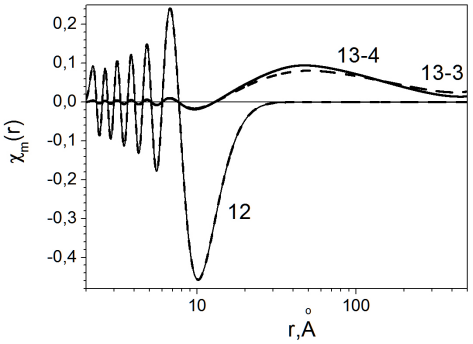

Table. The eigenvalues E_{12} and E_{13} (cm^{-1}) of the BVP in different intervals $r \in (1.5, r_{\max})$ with the BC of the second kind for different approximations of the tabulated potential $V(r)$, labelled by -1, -3, -4, and intervals of r variation.

	$r \in [1.5, 78]$		$r \in [1.5, 500]$	
mark	E_{12}	E_{13}	E_{12}	E_{13}
-1	-.3262890	—	-.3262890	—
-3	-.3262690	-0.0017990	-.3262690	-0.0001689
-4	-.3262626	-0.0018400	-.3262626	-0.0001957

Figure 2. The 12-th ($E_{12} = -0.326\ \mathrm{cm}^{-1}$) and 13-th ($E_{13} = -0.0001689\ \mathrm{cm}^{-1}$ labeled -3 or $E_{13} = -0.0001957\ \mathrm{cm}^{-1}$ labeled -4) eigenfunction $\chi_m(r) = r\Phi_m(r)$ vs. r for the vibrational spectrum of beryllium diatomic molecule.

approximation, has the form

$$\left(-\frac{\hbar^2}{2mDa\text{Å}^2}\left(\frac{1}{r^2}\frac{d}{dr}r^2\frac{d}{dr}\right)+\tilde{V}_L(\tilde{r})-\tilde{E}_{vL}\right)\tilde{\Phi}_{vL}(\tilde{r})=0, \quad \tilde{V}_L(\tilde{r})=\tilde{V}(\tilde{r})+\frac{\hbar^2}{2mDa\text{Å}^2}\frac{L(L+1)}{r^2}, \tag{1}$$

where L is the total angular momentum quantum number, $\hbar^2/(2Da)=1.685762920\cdot 10^{-7}$ Å, the reduced mass of beryllium is $m=M/2=4.506$, $\tilde{r}=r$ Å, the effective potential is $\tilde{V}(\tilde{r})$ in atomic units $aue=0.002194746314$ Å^{-1}, the energy is $\tilde{E}_{vL}$ cm^{-1}. The BVP for Eq. (1) was solved in the following units: the variable r is specified in (Å), the effective potential $V(r) = (2mDa\text{Å}^2 aue/\hbar^2)\tilde{V}(r\text{Å})=58664.99239\ \tilde{V}(r\text{Å})$ Å^{-2}, and the desired value of energy $E_{vL}=(2mDa\text{Å}^2/\hbar^2)\tilde{E}_{vL}$ in Å^{-2}, $\tilde{E}_{vL}=(1/0.2672973729)E_{vL}$ cm^{-1}.

In Ref.[3] the potential $V(r)$ (in cm^{-1}) (see Fig. 1) is given by the BO potential function marked as MEMO tabular values $\{V^M(r_i)\}_{i=1}^{76}$ in interval $r \in [r_1 = 1.5, r_{76} = 48]$Å. These tabular values were chosen to provide better approximation of the potential $V(r)$ by the fifth-order Lagrange interpolation polynomials (LIPs) of the variable r in subintervals $r \in [r_{5k-4}, r_{5k+1}]$, $k = 1, ..., 15$. Indeed, one can see that Fig. 1a displays smooth approximation till $r_{49} = 12$ where the approximate potential curve coincides with and crosses the asymptotic potential $V_{\text{as}}(r)$ given analytically by the expansions[9]

$$V_{\text{as}}(r)=58664.99239\tilde{V}_{\text{as}}(r), \quad \tilde{V}_{\text{as}}(r)=-\left(214(3)Z^{-6}+10230(60)Z^{-8}+504300Z^{-10}\right), \quad Z=r/0.52917. \tag{2}$$

This fact allows considering the interval $r \in [r_{\text{match}} \geq 12, \infty)$ as possible for using the asymptotic potential $V_{\text{as}}(r)$ at large r and executing conventional calculations based on tabular values of $V(r)$ in the finite interval $r \in [r_1, r{=}12]$ (see also[4]). However, the above MEMO tabular values have been calculated in the unusually larger interval $r \in [r_1, r{=}48]$ using special composite basis functions in different subintervals, taking into account both polarization and relativistic corrections DK-MRCI in the subinterval $r \in [r = 12, r = 48]$.[2] We note that the MEMO tabular values for $r \in \{r_{41} = 6.5, ..., r_{48} = 11\}$ are smaller than the asymptotic ones by $5.5 \div 6\%$, for $r = r_{51} = 14$ exceed the asymptotic ones by 8%, and beyond the interval $r \in [r_{40} = 6.0, ..., r_{52} = 15]$ the difference is more than 10%. Based on this fact, we consider three cases of approximation of this potential function in the extended interval marked by the key $K = -1$, -3 or -4.

At $K = -1$, the potential $V(r)$ in the subintervals $r \in [r_{5k-4}, r_{5k+1}]$, $k = 1, ..., 9$ was approximated by the fifth-order interpolation Lagrange polynomials of the variable r in the interval $r \in [r_1, r_{46} = 14]$. In the subinterval $r \in [r_e = r_{46} = 9, r_{\text{match}} = 14]$ we consider the approximation of the potential $V(r)$ by the fourth-order interpolation Hermite polynomial using the values of the potential $V(r)$ at the points $r = \{r_e = r_{46} = 9, r_{47} = 10, r_{48} = 11\}$ and the values of the asymptotic potential $V_{\text{as}}(r)$ and its derivative $dV_{\text{as}}(r)/dr$ at the point $r = r_{\text{match}} = 14$. In the $r \in [r_{\text{match}} = 14, \infty)$ the potential $V(r)$ is approximated by the asymptotic expansion (2). This approximation has been accepted in our paper.[7]

Below we consider also approximation of $V(r)$ in the cases of $K = -3$ and $K = -4$ to show what happens if we use nonstandard behavior of potential $V(r)$ in the interval $r \in [r_e^L > 12, r_{\text{match}})$ where it is lower than the

standard asymptotic potential $V_{\rm as}(r)$, Eq. (2). At $K=-3$ and $K=-4$, the potential $V(r)$ in the subintervals $r\in[r_{5k-4},r_{5k+1}]$, $k=1,...,10$ was approximated by the fifth-order interpolation Lagrange polynomials of the variable $r\in[r_1,r_{51}=19]$. At $K=-3$ and $K=-4$ in the extended interval $r\in[r_e^H,r_{\rm match}=100]$ the potential $V(r)$ is approximated using the values of the potential $V(r)$ at points $r=\{r_{55}=18,r_{67}=30,r_{76}=48\}$ and at points $r=\{r_{53}=16,r_{57}=20,r_{67}=30,r_{76}=48\}$ by means of the fourth– and fifth–order interpolation Hermite polynomials of the auxiliary variable $x=1/r$, i.e. the values of the potential $V(r(x))$ at the points $x=\{1/r_e=1/18,1/30,1/48,1/100\}$ for case $K=-3$ and at the points $x=\{1/r_e=1/16,1/20,1/30,1/48,1/100\}$ for case $K=-4$, respectively, and the value of the derivative $dV^{as}(r(x))/dx=-r^2dV^{as}(r)/dr$ of the asymptotic potential $V^{as}(r)$ at the point $x=1/100$, i.e. $r=100$. At $r\le r_e$ and $r\ge r_{\rm match}$ we use the same approximation as in the case $K=-1$.

The above approximations are specified in Å^{-2} as REAL*8 FUNCTION VPOT(K,R) of the variable R in (Å) and for $K=-1,-3,-4$ (see Appendix) and shown in the inset of Fig. 1. For comparison we show in Fig. 1 the potential function $V(r)$, its asymptotic expansion $V_{\rm as}(r)$ and the analytical potential functions $\tilde{V}_{an}(r)$ in a.u., proposed in Ref.[8] The MEMO potential function $V(r)$ is seen to have a minimum $-D_e$(FEM)=$V(R_e)$=-929.804cm^{-1} at the equilibrium point R_e=2.4534 Å and shifts above the analytic potential function $V_{\rm an}(r)$ in the vicinity of this point $-D_e$(Sheng)=$V_{\rm an}(R_e)$=-948.3cm^{-1}, while the analytic potential function $V_{\rm an}(r)$ lies above the MEMO potential function $V(r)$ in the interval $r\in(3.2,6.1)\cup(12.0,48.0)$. Moreover, the MEMO potential curve $V(r)$ goes below both the analytic potential curve $V_{\rm an}(r)$ and the asymptotic expansion $V_{\rm as}(r)$ at large values of r. So, the difference $V_{\rm as}(r)-V(r)$=0.00067Å^{-2} =0.0025cm^{-1} at the boundary point r=r_b=48 Å provides a suitable matching point r=$r_{\rm match}=100$ of $V(r)$ with $V_{\rm as}(r)$.

In the calculation presented below, we used the asymptotic expansion $V_{\rm as}(r)$ from (2) with which the matching of the tabulated potential $V(r)$ and the asymptotic potential $V_{\rm as}(r)$ was executed at $r=r_{\rm match}=100$ using REAL*8 FUNCTION VPOT(K,R) of the variable R in (Å) (see Appendix).

The BVP for Eq. (1) was solved using the FEM programs KANTBP 4M and ODPEVP on the finite element mesh $\Omega_1=\{1.50\ (n_g)\ 2.00\ (n_g)\ 2.42\ (n_g)\ 2.50\ (n_g)\ 3.00\ (n_g)\ 3.50\ (n_g)\ 4.00\ (n_g)\ 5.00\ (n_g)\ 6.00\ (n_g)\ 9.00\ (n_g)\ 14.00\ (n_g)\ 19.00\ (n_g)\ 24.00\ (n_g)\ 29.00\ (n_g)\ 38.00\ (n_g)\ 48.00\ (6n_g)\ r^{\max}\ge 48.00\}$ with the second-type or Neumann boundary conditions (BCs). In each of the subintervals (except the last one) the potential $V(r)$ was approximated by the LIP of the fifth order and $n_g=64$ finite elements were used. The last integrand was divided into $6n_g$ finite elements and the potential $V(r)$ was replaced with its asymptotic expansion (2). In the solution of the BVP at all finite elements of the mesh the local functions were represented by fifth-order LIPs.

In Table of Fig. 2 the first column presents the type of approximation of the tabulated potential $V(r)$ and its asymptotic expansion in extended intervals labelled -1, -3, -4. Note that the eigenvalues in the first row of this Table were obtained by solving the BVP in the extended intervals with the BCs of the second kind and provide the *lower estimate* $E_{12}=-0.3263\text{cm}^{-1}$ for the energy of the 12-th eigenvalue. As seen from the Table, the influence of the asymptotic expansions of $V(r)$ is essential only for the 13-th state with the energy close to the dissociation threshold ($E=0$) which does not support by asymptote labelled $1-1$. So, the third and the fourth row give *upper estimates* of the eigenenergy $E_{12}=-0.3263\text{cm}^{-1}$ and $E_{13}=-0.0002\ \text{cm}^{-1}$ in comparison with our results presented in the first row of the Table.

Figure 2 shows the 12-th ($E_{12}=-0.326\ \text{cm}^{-1}$) and 13-th ($E_{13}=-0.0001689\ \text{cm}^{-1}$ labeled -3 or $E_{13}=-0.0001957$ labeled -4) eigenfunction $\chi_m(r)=r\Phi_m(r)$ versus r for the vibrational spectrum of beryllium diatomic molecule, calculated using the program ODPEVP on the finite-element mesh Ω_1 at $r^{\max}=500.00$ with the LIP of the fifth order. One can see that the eigenfunction labelled $13-4$ decreases faster than the eigenfunction $13-3$ with increasing value of r, while the influence of different asymptotic behaviour of $V(r)$ labelled -1, -3 or -4 in the region $r>16$ on behavior of the eigenfunction $\Phi_{12}(r)$ is negligibly small. Note, that our calculation using the program implementing the Numerov method on the mesh (0,100) for the first 12 levels and (0,500) for the 13-th level with the mesh spacing 0.02 with Dirichlet BCs for $\chi_m(r)=r\Phi_m(r)$ differs from the FEM results only in the last significant digit. Thus, answering the question about the existence of the elusive 13-th vibrational bound state of diatomic beryllium molecule depends on the limited accuracy of the tabulated potential function in the region of $r>12$ and the matching point of nonstandard asymptotic expression of the potential function with the standard one.

Table 2. The vibrational-rotational bound states $-E_{vL}$ (in cm^{-1}) of beryllium diatomic molecule.

L	$v=0$	1	2	3	4	5	6	7	8	9	10	11
0	806.07	583.57	408.73	288.36	211.18	154.16	107.15	68.35	37.80	16.33	4.41	0.33
1	804.85	582.44	407.72	287.51	210.47	153.54	106.60	67.87	37.40	16.03	4.21	0.22
2	802.43	580.17	405.70	285.81	209.06	152.31	105.51	66.93	36.61	15.42	3.81	0.07
3	798.78	576.77	402.67	283.27	206.93	150.46	103.88	65.51	35.42	14.51	3.23	
4	793.93	572.24	398.64	279.88	204.11	148.00	101.72	63.62	33.84	13.31	2.48	
5	787.86	566.57	393.60	275.65	200.59	144.93	99.02	61.28	31.89	11.83	1.57	
6	780.59	559.79	387.57	270.60	196.38	141.27	95.79	58.48	29.56	10.09	0.56	
7	772.11	551.88	380.55	264.72	191.49	137.01	92.04	55.24	26.87	8.11		
8	762.43	542.85	372.54	258.04	185.93	132.16	87.78	51.56	23.85	5.91		
9	751.55	532.70	363.55	250.56	179.71	126.74	83.03	47.46	20.49	3.53		
10	739.47	521.45	353.60	242.29	172.84	120.76	77.78	42.96	16.84	1.02		
11	726.20	509.10	342.69	233.26	165.34	114.22	72.06	38.06	12.91			
12	711.74	495.65	330.84	223.48	157.23	107.15	65.87	32.79	8.75			
13	696.09	481.11	318.05	212.97	148.51	99.55	59.25	27.18	4.40			
14	679.27	465.50	304.35	201.76	139.21	91.45	52.20	21.25				
15	661.28	448.81	289.75	189.88	129.36	82.86	44.76	15.04				
16	642.12	431.07	274.27	177.35	118.97	73.81	36.94	8.58				
17	621.80	412.27	257.94	164.21	108.06	64.32	28.78					
18	600.34	392.44	240.77	150.49	96.67	54.42	20.31					
19	577.72	371.59	222.81	136.25	84.81	44.14	11.59					
20	553.98	349.72	204.07	121.51	72.53	33.51						
21	529.10	326.87	184.61	106.35	59.85	22.58						
22	503.11	303.05	164.46	90.81	46.82	11.40						
23	476.02	278.27	143.67	74.95	33.46							
24	447.82	252.56	122.33	58.84	19.83							
25	418.55	225.94	100.49	42.53								
26	388.20	198.45	78.27	26.09								
27	356.79	170.11	55.77	9.58								
28	324.34	140.96	33.18									
29	290.86	111.05	10.70									
30	256.36	80.42										
31	220.87	49.14										
32	184.41	17.28										
33	146.98											
34	108.63											
35	69.36											
36	29.21											

Table 1 presents the results of using FEM programs KANTBP 4M and ODPEVP to calculate 12 eigenvalues of beryllium diatomic molecule. Table 1 shows the eigenvalues calculated with ab initio modified (MEMO) expanded Morse oscillator (EMO) potential function[3] and the corresponding FEM approximation. In contrast to the original EMO function, which was used to describe the experimental (Exp) vibrational levels,[6] it has not only the correct dissociation energy, but also describes all twelve vibrational energy levels with the RMS error smaller than 0.4 cm^{-1}. The table also shows the results of recent calculation using the Morse long-range (MLR) function and Chebyshev polynomial expansion (CPE) alongside with the EMO potential function.[5] Similar results were obtained by Lesiuk et al.[4] The main attention in the optimization of the MLR and CPE functions was focused on their correct long-range behavior displayed in Fig. 1. However, there are some problems with the quality of the MLR and CPE potential curves.[3] As a consequence, one can see from the table, that the corresponding results provide *a lower estimate* while FEM and MEMO results give *an upper estimate* for the discrete spectrum of the diatomic beryllium molecule.

The potential functions $V_L(r)$ from $L=0$ to $L=36$ support $37+33+30+28+25+23+20+17+14+11+7+3 = 248$ vibrational–rotational levels $-E_{vL}$ presented in Table 2. Figure 3a shows also the rotational-vibrational spectrum E_{vL} (in cm^{-1}) of the beryllium diatomic molecule vs L. These functions $V_L(r)$ are displayed in Fig. 3d at $L=0,...,36$ with the step 4. One can see that the potential $V_L(r)$ at $L=0$, $L=1$ and $L=2$ supports 12 vibrational energy levels.

The complex eigenenergies $E^M_{Ln} = \Re E^M_{Ln} + \imath \Im E^M_{Ln}$, (in cm^{-1}) of rotational–vibrational metastable states, where n is the number of states at fixed value of L, of beryllium diatomic molecule are shown in Table 3. Their real parts $\Re E^M_{Ln}$ are displayed in Fig. 3b in comparison with the eigenenergies E_{vL} of vibrational–rotational bound states Fig. 3a. The BVP for Eq. (1) was solved by the FEM programs on the above finite element mesh Ω_1 with mixed BVPs, i.e. the Neumann BC at the left point r_1 of the finite interval $r \in [r_1, r^{\max}]$ and the third-type or Robin BC at the right point r_{max} using the corresponding asymptotic solution $\Phi^{M(\mathrm{as})}_{Ln}(r)$ in

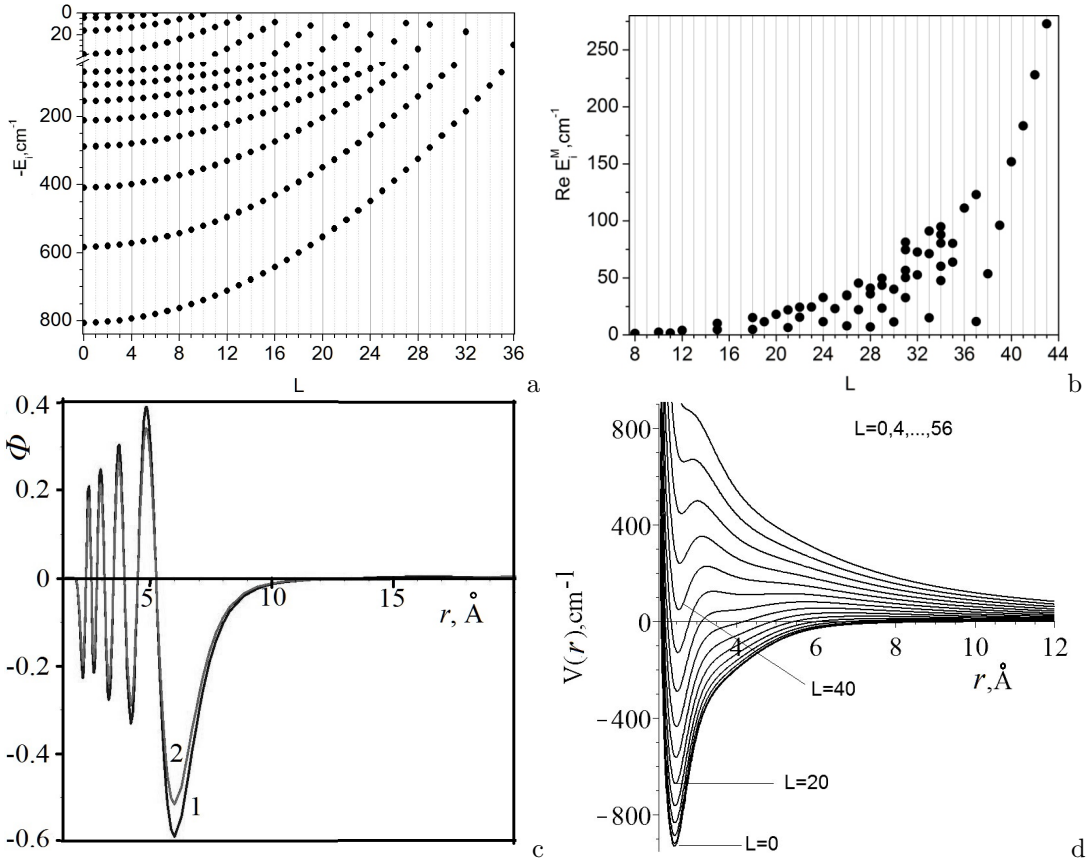

Figure 3. The eigenenergies E_{vL} of vibrational–rotational bound states (a) and real parts of complex eigenenergies $\Re E^M_{Ln}$ of rotational–vibrational metastable states (b) The real (1) and imaginary (2) parts of eigenfunction $\Phi_{1L=25}(r)$ with angular momentum $L = 25$ of metastable state with complex energy $E_{1L=25} = 22.99 - 3.1E - 11i$ (cm^{-1}) of rotation-vibration spectrum of Be_2 molecule (c), The potential functions $V_L(r)$ at $L = 0, 4, ..., 56$ (c).

Table 3. The rotational–vibrational metastable states $E^M_{Ln} = \Re E^M_{Ln} + \Im E^M_{Ln}$ (in cm^{-1}) of beryllium diatomic molecule.

L	n	$\Re E^M_{Ln}$	$-\Im E^M_{Ln}$	L	n	$\Re E^M_{Ln}$	$-\Im E^M_{Ln}$	L	n	$\Re E^M_{Ln}$	$-\Im E^M_{Ln}$	L	n	$\Re E^M_{Ln}$	$-\Im E^M_{Ln}$
8	1	1.37	8.0E-6	24	1	11.48	1.9E-15	31	1	32.62	8.4E-19	35	1	63.86	3.9E-4
10	1	2.44	1.2E-5	24	2	32.84	1.2E-8	31	2	50.19	6.2E-5	35	2	80.25	6.9E-11
11	1	1.55	2.3E-9	25	1	22.99	3.1E-11	31	3	56.53	3.7E-8	36	1	111.28	8.4E-10
12	1	4.03	4.9E-6	26	1	7.99	3.3E-19	31	4	74.71	1.0E-3	37	1	11.78	1.4E-23
15	1	4.59	1.7E-5	26	2	34.35	1.6E-10	31	5	81.27	1.3E-4	37	2	122.96	1.2E-10
15	2	10.13	3.0E-5	26	3	34.94	5.0E-8	32	1	52.66	1.8E-10	38	1	53.59	5.1E-23
18	1	4.78	1.6E-13	27	1	22.03	1.3E-12	32	2	72.62	2.7E-5	39	1	96.16	9.8E-19
18	2	15.15	2.3E-5	27	2	45.34	4.8E-7	33	1	15.02	3.6E-17	40	1	151.81	4.6E-10
19	1	11.51	3.2E-8	28	1	6.96	2.2E-18	33	2	71.13	7.6E-8	41	1	183.40	2.4E-13
20	1	17.97	3.5E-6	28	2	35.99	1.2E-12	33	3	91.09	1.2E-5	42	1	227.98	1.4E-13
21	1	6.40	1.2E-15	28	3	41.03	1.9E-7	34	1	47.64	6.4E-19	43	1	272.84	5.6E-15
21	2	21.97	2.7E-5	29	1	23.51	4.1E-15	34	2	60.15	6.4E-4	44	1	317.58	4.8E-18
22	1	15.49	5.2E-10	29	2	43.45	4.6E-7	34	3	80.43	1.6E-4				
22	2	24.34	5.9E-7	29	3	49.66	2.7E-7	34	4	87.94	4.6E-5				
23	1	24.44	5.8E-9	30	1	11.35	7.8E-22	34	5	94.90	2.0E-6				
				30	2	40.05	2.1E-14								

the form of an outgoing wave.[13] An example of the complex-valued eigenfunction $\Phi^{M}_{L=25n=1}(r)$ is shown in Fig. 3c. The potential functions $V_L(r)$ at $L = 8, ..., 44$ supported this set of metastable states. These functions are plotted in Fig. 3d at $L = 8, ..., 56$ with the step 4. For $L > 0$ the potential functions at large r decrease proportionally to r^{-2} and at $L < 37$ have the form of a potential well with a minimum below the dissociation threshold D_0, while at $L > 37$ the potential well has a minimum above the dissociation threshold. The height of the centrifugal barrier increases with increasing L, but its width at the dissociation threshold energy is infinite. With increasing energy, the effective width of the barrier decreases. At low L the height of the barrier is very small, and depends on a square of the potential well, both in the presence and in the absence of a metastable state, i.e., shape resonances occur, is possible. These resonance are observed at $L < 18$, the width of such states depends on the real part of the energy and at low energies can be extremely small. Further, at $L > 18$, up to five vibrational metastable states can fit between the dissociation threshold and the top of the barrier at some fixed values of L, in particular at $[5(L = 31), 5(L = 34)]$. At $L > 37$ the potential well has a minimum above the dissociation threshold and the effective barrier width, width and depth of the well decrease, and at $L > 44$ the levels are absent in the well, and at $L > 54$ the potential well disappears.

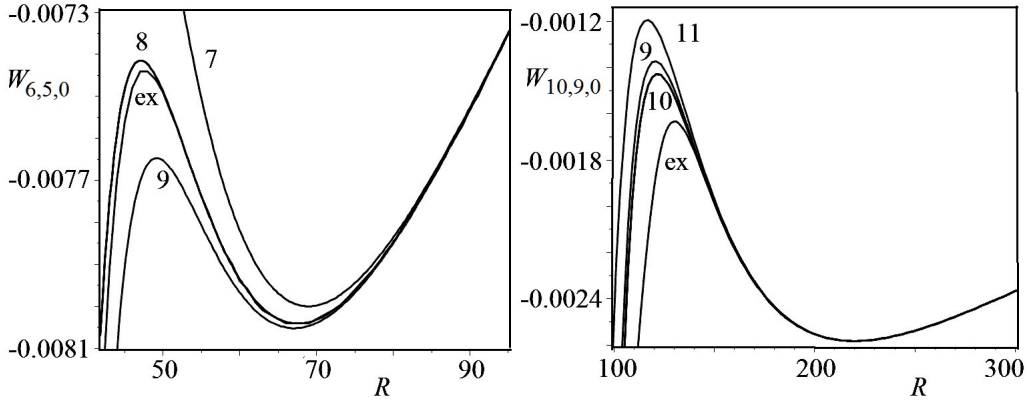

Figure 4. The BO potential curves $W_{N,N-1,0}(R)$ at $N = 6$ and $N = 10$: ex is the numerical values and their perturbation approximations of specified order k.

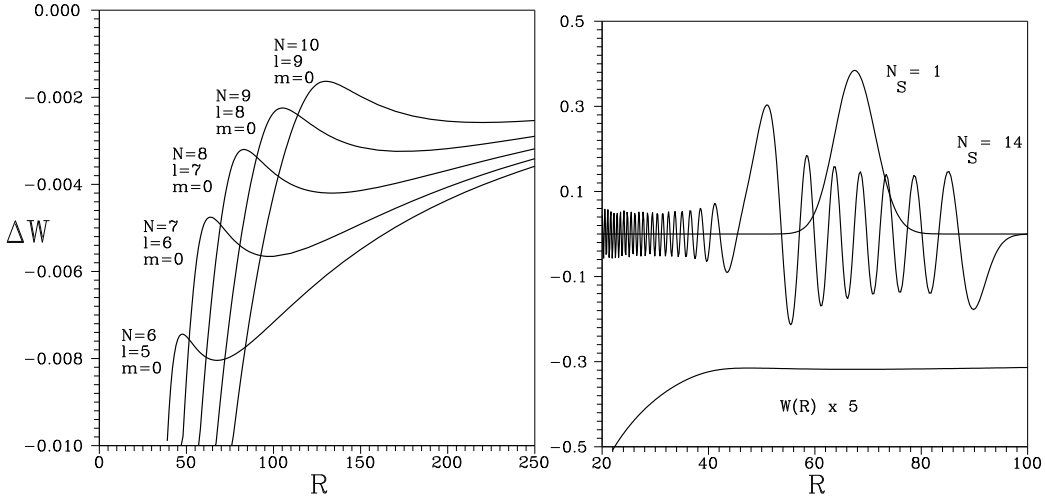

Figure 5. The low part of Rydberg set of Born-Oppenheimer potentials $\Delta W_{N,N-1,0}(R) = W_{N,N-1,0}(R) - E_N(+\infty)$ of antiprotonic helium atom (left panel) and eigenfunctions $\chi_{vi}(R) = R^2\Phi_{vi}(R)$ of the Rydberg antiprotonic helium atom $(i = \{N = 6, l = 5, m = 0\})$ with vibrational numbers $v = 0$ and $v = 13$, $N_s = v + 1$ (right panel).

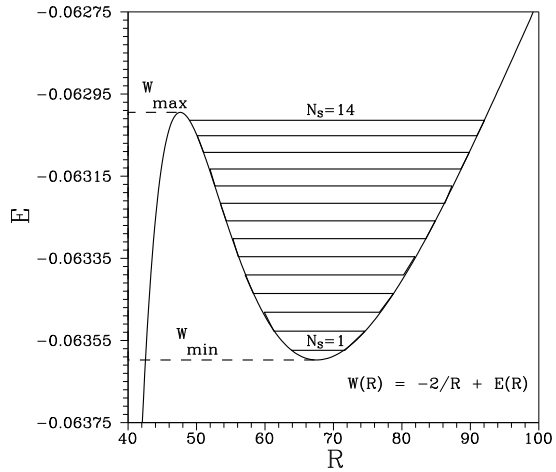

N_s	$E, 10^{-2}$a.u.	N_s	$E, 10^{-2}$a.u.
1	-6.357 395	8	-6.325 872
2	-6.352 732	9	-6.321 596
3	-6.348 121	10	-6.317 386
4	-6.343 562	11	-6.313 249
5	-6.339 057	12	-6.309 203
6	-6.334 605	13	-6.305 154
7	-6.330 210	14	-6.301 406

Figure 6. Energy levels in asymmetric outer oscillator well $W_{Nlm}(R)$ (N=6, l=5, m=0). The quasiequidistant vibrational spectrum $E_{vi}, v = 0, ..., 13$, $N_s = v + 1$, of the antiprotonic helium atom ($i = \{N = 6, l = 5, m = 0\}$) supported by the outer well $W_i(R)$ at which it is approximated by formula $E_v^{approx} = W_{min} + C_v(W_{max} - W_{min})$, $C_v = 0.04 + 0.07v$.

3. WEAKLY BOUND RYDBERG STATES OF ANTIPROTONIC HELIUM

We continue to study metastable states of the $\bar{p}\mathrm{He}^+$ atomcule,[15–17] as benchmark calculations for the FEM programs and symbolic program POINTFIELD[14] for calculations of asymptotic expansions of potential function of the helium ion He^+ in the Coulomb field of point charge of $\bar{p}$. We focus our attention at the new weakly bound Rydberg states[18] supported by the asymmetric outer oscillator well of adiabatic potential of the antiprotonic helium atom. To estimate the real part of energy E_{iv} and the corresponding wave function $\Phi_{vi}(R)$ of these vibrational states supported by the outer well, it is needed to solve the BVP for the radial SOODE on a semiaxis in atomic units (au)

$$\left[\frac{1}{2\mu}\frac{1}{R^2}\frac{d}{dR}R^2\frac{d}{dR} + (E_{iv} - W_i(R))\right]\Phi_{iv}(R) = 0, \quad W_i(R) \equiv= Z_{\bar{p}}Z_{He}/R + E_{n_\xi,n_\eta,m}(R),$$

where μ is the reduced mass $\mu = M_{He}m_{\bar{p}}/M_{He} + m_{\bar{p}}$, $m_{\bar{p}} = 1836.1527m_e$, $M_{^4He} = 7294.299m_e$, $W_i(R)$ is the Born-Oppenheimer(BO) potential curve consisting on a sum of the attractive Coulomb potential $Z_{\bar{p}}Z_{He}/R = -2/R$ between antiproton and helium nucleus, and the eigenvalues $E_i(R) \equiv E_{n_\xi,n_\eta,m}(R) = E_{Nlm}(R)$ of the two-center Coulomb problem in spheroidal coordinates $\xi = (r_{\bar{p}} + r_{He})/R$ and $\eta = (r_{\bar{p}} - r_{He})/R$ with distance R between focuses with charges $Z_{\bar{p}} = -1$ and $Z_{He} = +2$. The solutions $\Phi_{vi}(R)$ are subjected to the second type BC and normalization condition in the appropriate finite interval.

The analysis of the asymptotic behavior of the Born-Oppenheimer potentials $W_i(R) \equiv W_{n_\xi,n_\eta,m}(R)$ at large $R>>2N/Z_{He}$ with the accuracy $O((RZ_{He}/N)^{-15})$ calculated using the program POINTFIELD implemented in REDUCE[14] and presented here with the accuracy $O((RZ_{He}/N)^{-3})$

$$W_i(R) \equiv W_{n_\xi,n_\eta,m}(R)=-(Z_{He})^2/(2N^2) + Z_{\bar{p}}(Z_{He}-1)/R + 3N(n_\xi - n_\eta)Z_{\bar{p}}/(2Z_{He}R^2),$$

revealed the existence of the local minimum of $W_i(R)$ in the Rydberg electronic state $|i>$ characterized by the following set of the spheroidal quantum numbers: $n_\xi = 0$, $n_\eta = l - |m| = N - 1$, $m = 0$, where $N = n = n_\xi + n_\eta + |m| + 1$, presented by the corresponding asymptotic expansion

$$W_i(R) = W_{n_\xi=0,n_\eta=n,m=0}(R) = W_{n,n-1,0}(R) = -(Z_{He})^2/(2n^2) - 1/R + (3/2)n(n-1)/(2R^2)$$
$$+n^2(n-1)(5n-7)/(8R^3) + 3n^3(21n^3 - 97n^2 + 126n - 56)/(128R^4) + 3n^4(n-1)(27n^3 - 221n^2 + 332n - 200)/(256R^5)$$
$$+n^5(-9804 + 29200n - 36369n^2 - 6450n^4 + 22974n^3 + 209n^5)/(2048R^6)$$
$$-3n^6(-7456 + 24074n - 33750n^2 - 11077n^4 + 26085n^3 + 1904n^5 + 78n^6)/(2048R^7)$$
$$-3n^7(11850n^7 + 79513n^6 - 879361n^5 + 2947864n^4 - 5483264n^3 + 6245400n^2 - 4106160n + 1197728)/(131072R^8)$$
$$-n^8(19805n^8 + 40500n^7 - 1449069n^6 + 6740937n^5 - 16842998n^4 + 27126213n^3 - 28404888n^2 + 17622540n - 4909776)/(65536R^9)$$

Table 4. The positions $R_N^{\max}$ and $R_N^{\min}$ and maximum and minimum values of potential functions $W_{N,N-1,0}^{\max}$ and $W_{N,N-1,0}^{\min}$ vs the order k of perturbation theory compared to numerical ones, respectively. The numerical values (num) are given in last row.

	$n=6$				$n=10$			
k	$R_{\max}$	$R_{\min}$	$W_i(R_{\max}^{\text{num}})$	$W_i(R_{\min}^{\text{num}})$	$R_{\max}$	$R_{\min}$	$W_i(R_{\max}^{\text{num}})$	$W_i(R_{\min}^{\text{num}})$
1			-0.076550	-0.070357			-0.027684	-0.02454979
2		45.000	-0.066632	-0.065427		135.00	-0.023698	-0.02315250
3		67.873	-0.061843	-0.063749		205.58	-0.021503	-0.02269688
4		72.928	-0.060128	-0.063325		223.43	-0.020482	-0.02257130
5	3.108	72.705	-0.060230	-0.063343		225.88	-0.020255	-0.02255481
6	27.641	70.930	-0.061178	-0.063460	48.78	224.08	-0.020496	-0.02256520
7	40.542	68.965	-0.062241	-0.063552	90.84	221.78	-0.020914	-0.02257587
8	47.089	67.550	-0.062973	-0.063596	111.82	220.28	-0.021289	-0.02258153
9	49.140	67.073	-0.063227	-0.063607	120.70	219.69	-0.021498	-0.02258340
10	48.032	67.269	-0.063099	-0.063603	121.82	219.64	-0.021525	-0.02258354
11	44.085	67.583	-0.062815	-0.063597	116.74	219.75	-0.021435	-0.02258326
12		67.748	-0.062605	-0.063594		219.83	-0.021329	-0.02258307
13		67.749	-0.062604	-0.063594		219.85	-0.021290	-0.02258302
14	45.132	67.659	-0.062803	-0.063595	110.03	219.83	-0.021351	-0.02258306
num	47.630	67.558	-0.062994	-0.063597	130.14	219.79	-0.021633	-0.02258315

$$-3n^9(117040n^9-2952n^8-16504269n^7+100530674n^6-316661506n^5+664836933n^4-977982168n^3$$
$$+967987480n^2-575546304n+154673488)/(2097152R^{10})$$
$$+3n^{10}(76524n^{10}-700510n^9+20875452n^8-142168095n^7+517892481n^6-1304977702n^5+2465232776n^4$$
$$-3428443356n^3+3265843056n^2-1880625904n+490950784)/(2097152R^{11})$$
$$+n^{11}(28143720n^{11}-295156752n^{10}+3349874451n^9-21716721180n^8+83354178568n^7-229079358171n^6+504392770058n^5$$
$$-896261311356n^4+1205199562128n^3-1118072631120n^2+628020672288n-160078452288)/(67108864R^{12})$$

that realizes at the point $R_N^{\min} \simeq (3N-3+\sqrt{39N^2-90N+51})N/4$. This asymptotic expansion has been calculated with accuracy $O((RZ_{He}/N)^{-13})$ that agrees with the accuracy of the order of 0.0001 a.u. and 0.000004 a.u. with the numerical results $W_{N,N-1,0}^{\max}$ and $W_{N,N-1,0}^{\min}$ in the vicinities of $R_N^{\max}$ and $R_N^{\min}$, respectively. In Table 4 we show the convergence of positions $R_N^{\max}$ and $R_N^{\min}$ and values of maximum and minimum potential functions $W_{N,N-1,0}^{\max}$ and $W_{N,N-1,0}^{\min}$ to numerical ones, respectively. The asymptotic type convergence of PT series $W_{N,N-1,0}(R)$ at $N=6$ and $N=10$ versus order k is illustrated in Fig. 4. Fig. 5 shows the existence of the such local minimum and corresponding outer wells which support the loosely bound vibrational states of the antiproton. For convenience the value $\Delta W_i(R) = W_i(R) - E_i(+\infty)$, counted on threshold energy $E_N(+\infty) = E_N^{He^+} = -(Z_{He})^2/(2N^2)$ of separated atom (positive ion He^+) is demonstrated at $N=6,7,8,9,10$. As an example, the potential $W_i(R)$ is considered for the spherical quantum numbers $i=\{N=6,l=5,m=0\}$. The local maximum is $W_{max}=-0.0629946$ at $R_{max}\simeq 47.6$ and the local minimum is $W_{min}=-0.0635974$ at $R_{min}\simeq 67.6$. In this outer well the fourteen quasi-equidistant energy levels shown in Fig. 6 have been recalculated on the finite element mesh $\Omega_2 = \{0.01(19)0.2(20)0.6(10)0.9(15)1.5(10)2(10)2.6(20)4(20)5.6(24)8(32)12(24)15.6(22)20(20)24(30)33(14)$ $40(4)44(10)59(15)80(12)98(11)120\}$ with the help of the above FEM algorithm and program on the uniform grid with 20 Lagrange elements of 6th-order and second-type BCs. The FEM results differ only in the last significant digit from those calculated earlier by Newton method with forth-order finite difference approximation.[16,17] The wave functions $\Phi_{iv}(R)$ at $N_s = v+1 = 1$ and $N_s = v+1 = 14$ without nodes and with thirteen nodes, respectively, supported by the outer well in the BO potential $W_i(R)$ at $i=\{N=6,l=5,m=0\}$ converging to $N=6$ threshold energy are shown on Fig. 5. Thus, there is a countable set $N=6,7...$ of the asymmetric outer oscillator wells of BO potential curves $W_{N,N-1,0}(R)$, converging to the Coulomb threshold $E=0$ and supporting subsets of the vibrational weakly bound Rydberg states of antiprotonic helium atoms.

4. CONCLUSION

The efficacy of the applied programs is demonstrated by the calculations of twelve eigenenergies of the vibrational bound states of the diatomic beryllium molecule with the required accuracy in comparison with those known from literature, as well as the vibrational-rotational spectrum bound states and rotational-vibrational spectrum of sharp metastable states with complex eigenenergies, that are important for laser spectroscopy.

It is shown that the elusive 13th vibrational bound state of diatomic beryllium molecule is supported by the approximations of the tabulated potential function calculated with limited accuracy FUNCTION VPOT(K,R)

at $K = -3$ and $K = -4$, which lie below the conventional asymptotic expansion (2) in the region of $r > 12$. To understand it, the new high-accuracy ab initio calculations of the tabulated potential function and its asymptotic expansions are needed. It will be similar to the above accuracy of the numerical and asymptotic calculations for antiproton Helium atomcule. Independent on answering this question, we hope that FUNCTION VPOT(K,R) provides a useful tool for further study of approximations of the tabulated potential function and modeling calculations of the weakly bound states with eigenenergies close to the dissociation threshold.

It is shown that there is a countable set $N = 6, 7...$ of the asymmetric outer oscillator wells of BO potential curves $W_{N,N-1,0}(R)$ that converge to the Coulomb threshold $E = 0$ and support some subsets of the weakly bound Rydberg states of antiprotonic helium atoms. A possible role of these states in the formation mechanism of antiprotonic helium atoms is an interesting question for laser spectroscopy experiments.[19,20]

Appendix

```
 REAL*8 FUNCTION VPOT(K,R)
 REAL*8 R
 IF ( R .LT. 0.200D1) THEN
 VPOT = -25773.7109044290317516659D0*R
#+45224.0477977149109075999D0
#+11630.140936626390269198OD0*(R-1.50D0)**5
#-21410.9944579041874319967D0*(R-1.50D0)**3
#-6655.693014152965377936220*(R-1.50D0)**4
#+37646.6374905803929755811D0*(R-1.50D0)**2
 ELSEIF ( R .LT. 0.242D1) THEN
 VPOT = -3104.29731660146789925758D0*R
#+6567.966778351872377464140
#+145901.6375574369778443890*(R-2.00D0)**5
#+70890.0501932798636244675D0*(R-2.00D0)**3
#-178091.8917222178502898310*(R-2.00D0)**4
#-5215.0146584048034837183 3D0*(R-2.00D0)**2
 ELSEIF ( R .LT. 0.250D1) THEN
 VPOT = -87.46232242497922474125370*R
#-35.472249302812032254166 2D0
#-5122452.98252855176907985D0*(R-2.42D0)**5
#-37267.2557427451395256506D0*(R-2.42D0)**3
#+767538.5767238103685648740*(R-2.42D0)**4
#+1940.263762599047254290590*(R-2.42D0)**2
 ELSEIF ( R .LT. 0.300D1) THEN
 VPOT =95.54864159324161815881380*R
#-485.0096800385580342540340
#-559.7911788828559591744890*(R-2.50D0)**5
#-2399.4966669849129417965 6D0*(R-2.50D0)**3
#+2045.3678146438074587558 7D0*(R-2.50D0)**4
#+1039.1615814486574992629 2D0*(R-2.50D0)**2
 ELSEIF ( R .LT. 0.350D1) THEN
 VPOT = 181.68044562399449303416 3D0*R
#-673.2097660666176843404880
#-42.137572965180420838417 6D0*(R-3.00D0)**5
#+154.527717281912104793036D0*(R-3.00D0)**3
#-2.644214535118518744133 50D0*(R-3.00D0)**4
#-224.971347436273044312400D0*(R-3.00D0)**2
 ELSEIF ( R .LT. 0.400D1) THEN
 VPOT = 58.217063459233166714662 8D0*R
#-279.4968632523890857743200
#+16.300219686791840830204 5D0*(R-3.50D0)**5
#+60.280795675586126123826 7D0*(R-3.50D0)**3
#-47.226008187610582500000 0D0*(R-3.50D0)**4
#-47.294069698494169774818 1D0*(R-3.50D0)**2
 ELSEIF ( R .LT. 0.500D1) THEN
 VPOT =37.543374038277994102581 4D0*R
#-203.532767180257088384326D0
#+1.579334468059034453095 67D0*(R-4.00D0)**5
#+2.065367207979806432193 89D0*(R-4.00D0)**3
#-3.909139781853220130188 78D0*(R-4.00D0)**4
#-6.721754829773764844812 39D0*(R-4.00D0)**2
 ELSEIF ( R .LT. 0.600D1) THEN
 VPOT = 22.474942508881279992695 0D0*R
#-135.176802468861661924475D0
#-1.746327236454219349731 76D0*(R-5.00D0)**5
#-1.139106256366595009035 84D0*(R-5.00D0)**3
#+3.465515463834369153125 00D0*(R-5.00D0)**4
#-8.232976581699479347991 79D0*(R-5.00D0)**2
 ELSEIF ( R .LT. 0.900D1) THEN
 VPOT = 8.254463692501029690433 26D0*R
#-57.506824181266084664529 5D0
#+0.262554831228989391666862D-1*(R-6.00D0)**5
#+1.525957970033408020694 35D0*(R-6.00D0)**3
#-.302331762133111382686686D0*(R-6.00D0)**4
#-4.495464781655764157778 27D0*(R-6.00D0)**2
 ELSEIF ( R .LT. 0.1400D2) THEN
 VPOT = 11.385941234992376680396136937226D0*R
#-37.683304037819782698889968642231D0
#-1.303698811270540117575840166184 9D0*R**2
#+0.667546754803633073341801012861 4D-1*R**3
#-0.128615773754869182131374853976 57D-2*R**4
 ELSEIF(K=-4.AND.R.GT.16.D0) THEN
 VPOT=
#-0.132193335030019031906 8657998418 8D-2
#+0.315523537022625984561019625008 8D0/R
#-24.234314428857210703372495183184D0/R**2
#+671.286339759808331535216682069 0D0/R**3
#-8327.631687799952969848898504310 6D0/R**4
#+18433.767140948904286850064317 50D0/R**5
 ELSEIF(K=-3.AND.R.GT.18.D0) THEN
 VPOT=0.2813838028222176327014816866601 46D0/R
#-0.120373330899685144960823947904 73D-2
#-5258.380030078162840594078721806 6D0/R**4
#-20.682311196377164089738717232 25D0/R**2
#+510.434177349838364771384760384 11/R**3
 ELSEIF ( R .LT. 0.1900D2) THEN
 VPOT = 0.161133498108317784754988D-1*R
#-.268024960190735889896984D0
#-0.812473449648760055000041D-4*(R-14.00D0)**5
#-0.225620615273081523000047D-2*(R-14.00D0)**3
#+0.821018692659649454583372D-3*(R-14.00D0)**4
#-0.103596828074647247458354D-2*(R-14.00D0)**2
 ELSE
 Z=R/0.52917D0
 VPOT = -( 214.D0/Z**6+10230.D0/Z**8
# +504300.D0/Z**10)
 ENDIF
 VPOT =58664.99239D0*VPOT
 RETURN
 END
```

REFERENCES

1. Patkowski, K., Špirko, V., and Szalewicz, K. "On the elusive twelfth vibrational state of beryllium dimer, Science 326, 1382-1384 (2009)
2. Mitin, A.V. "Ab initio calculations of weakly bonded He_2 and Be_2 molecules by MRCI method with pseudo-natural molecular orbitals, Int. J. Quantum Chem. 111 2560–2567, (2011).

3. Mitin, A.V. "Unusual chemical bonding in the beryllium dimer and its twelve vibrational levels, Chem. Phys. Lett. 682, 30-33 (2017)
4. Lesiuk, M., Przybytek, M., Balcerzak, J.G., Musial, M. Moszynski, R. "Ab initio potential energy curve for the ground state of beryllium dimer, J. Chem. Theory Comput. 15, 2470-2480 (2019)
5. Meshkov, V.V., Stolyarov, A.V., Heaven, M.C., et al. "Direct-potential-fit analyses yield improved empirical potentials for the ground $X^1\Sigma_g^+$ state of Be_2, J. Chem. Phys. 140, 064315-1-8 (2014)
6. Merritt,J.M., Bondybey, V.E., Heaven, M.C. "Beryllium dimer – caught in the act of bonding, Science 324 (5934), 1548-1551 (2009)
7. Gusev, A., Chuluunbaatar, O., Vinitsky, S., et al. "On rotational-vibrational spectrum of diatomic beryllium molecule, Proceedings of SPIE, 11066, 1106619 (2019)
8. Sheng, X.W., Kuang, X.Y., Li, P., Tang, K.T. "Analyzing and modeling the interaction potential of the ground-state beryllium dimer, Phys. Rev. A 88, 022517 (2013)
9. Porsev S.G., Derevianko, A. "High-accuracy calculations of dipole, quadrupole, and octupole electric dynamic polarizabilities and van der Waals coefficients C_6, C_8, and C_{10} for alkaline-earth dimers, JETP, 102, 195-205 (2006)
10. Chuluunbaatar, O., Gusev, A.A., Vinitsky, S.I., Abrashkevich, A.G. "ODPEVP: A program for computing eigenvalues and eigenfunctions and their first derivatives with respect to the parameter of the parametric self-adjoined Sturm-Liouville problem, Comput. Phys. Commun. 181, 1358-1375 (2009)
11. http://wwwinfo.jinr.ru/programs/jinrlib/kantbp4m/indexe
12. Gusev, A.A., Chuluunbaatar, O., Vinitsky, S.I., et al. "Symbolic-numerical solution of boundary-value problems with self-adjoint second-order differential equation using the finite element method with interpolation Hermite polynomials, Lecture Notes in Computer Science 8660, 138-154 (2014)
13. Gusev, A.A., Hai, L.L., Chuluunbaatar, O., et al. "Symbolic-numeric solution of boundary-value problems for the Schrodinger equation using the finite
14. Gusev, A.A., Samoilov, V.N., Rostovtsev, V.A., Vinitsky, S.I. "Symbolic algorithms of algebraic perturbation theory: hydrogen atom in the field of distant charge, Proc. of Fourth Workshop on Computer Algebra in Scientific Computing, (Konstanz, September 22 - 26, 2001), CASC-2001, Eds. V.G. Ganzha, E.W. Mayr, E.V. Vorozhtsov, 309-322 (Springer-Verlag, 2001)
15. Derbov, V.L., Melnikov, L.A., Umansky, I.M., Vinitsky, S.I. "Multipulse laser spectroscopy of measurement and control of the metastable state populations, Phys. Rev. A 55, 3394-3400 (1997); Proc. SPIE 4243, 131-138 (2001)
16. Pavlov, D.V., Puzynin, I.V., Vinitsky, S.I. "Discrete spectrum of two-center problem of $\bar{p}He^+$ atomcule, [Preprint JINR E4-99-141, JINR], Dubna, 1999
17. Puzynin, I.V., Boyadjiev, T.L., Vinitsky, S.I., et al. "Methods of computational physics for investigation of models of complex physical systems, Physics of Particles and Nuclei 38, 70-116 (2007)
18. Richter K., Rost, J.-M., Thürwächter, R., et al. "New state of binding of antiprotons in atoms, Phys.Rev. Lett. 66, 149-152 (1991)
19. Hayano, R.S., Hori, M., Horvath, D., Widmann, E. "Antiprotonic helium and CPT invariance, Rep. Prog. Phys. 70, 1995-2065 (2007)
20. Kobayashi, T., Barna, D., Hayano, R.S., et al. , "Laser spectroscopic study on the highly excited states of antiprotonic helium, JPS Conf. Proc. 6, 030073 (2015).